Nanorod Synthesis

DOI: 10.1002/anie.201001822

Palladium Nanoparticle Catalyzed Conversion of Iron Nanoparticles into Diameter- and Length-Controlled Fe_2P Nanorods**

Heonjo Kim, Youngjoo Chae, Duck Hyun Lee, Minsik Kim, Jiyoung Huh, Youngki Kim, Hyunjin Kim, Hyun Jung Kim, Sang Ouk Kim, Hionsuck Baik, Kihang Choi, Jong Seung Kim, Gi-Ra Yi, and Kwangyeol Lee**

Nanoparticles and their composites hold great promise for advances in bio-, energy-, and environment-related fields. The properties of nanoparticles depend on composition, phase, dimension, and exposed crystal facets, and thus control over these parameters is crucial for nanoparticles to have desired properties. The process of nanoparticle formation is affected by various kinetic and thermodynamic parameters, which are determined by the intricate interplay of precursors, surfactants, and reaction temperature.[1–3] While variation of surfactant and reaction temperature has been a preferred approach for synthesis of new nanoparticles, more exotic methods, namely, elemental exchange,[4] doping-assisted kinetic control,[5] surface-stabilization by nonsurfactants,[6] epitaxial growth,[7] and etching,[8] are being developed to fine-tune nanocrystal growth and to overcome the dearth of precursors. While all of these ingenuous approaches enhance our understanding of nanocrystal growth and afford new nanomaterials, efforts to find new precursors should be continued for further advances in nanoscience.

We previously reported that soluble Pd^0 species, derived from [Pd(acac)$_2$] (acac = acetylacetonate), can catalyze etching of Fe_3O_4 nanoparticles to form soluble Fe species.[9] Thus, nanoparticles, although generally considered to be stable, can be disintegrated under suitable conditions to form hitherto-unknown precursors and, ultimately, novel nanostructures. We further investigated this possibility of utilizing nanoparticles as a source of new precursors, and discovered that catalytic Pd nanoparticles could transform Fe nanoparticles into magnetic Fe_2P nanorods. Synthetic routes to magnetic metal phosphides have been actively pursued in recent years due to their ferromagnetism, magnetoresistance, and magnetocaloric effects.[10] Surprisingly, the diameter and length of Fe_2P nanorods in our study are determined by the Pd nanoparticle diameter and Pd/Fe ratio, respectively. No dimensional similarity between the diameters of the Fe_2P nanorods and the precursor Fe nanoparticles was observed. Herein we report a completely unexpected dual role of the Pd nanoparticle as a catalyst for formation of an Fe precursor by destabilizing Fe nanoparticles and as a dimension-controlling catalytic center for Fe_2P nanorod growth.

In a typical synthesis, a sonicated slurry of Fe nanoparticles[11] (ca. 14 nm, 25 mg) in oleylamine (OA, 7 mL) and trioctylphosphine (TOP, 1 mL) was prepared in a 100 mL Schlenk tube equipped with a bubbler. A slurry of Pd nanoparticles[12] (3.5, 4.2, or 4.9 nm in diameter; 2 and 0.5 mg for formation of short and long Fe_2P nanorods, respectively) in OA (2 mL) was added to the above slurry, and the reaction mixture was placed under vacuum for 2 h. The Schlenk tube was purged with Ar (99.999 %) for 30 min, and then heated at 317 °C in an oil bath for 14 h under an Ar blanket (passage to the bubbler is shut off, and a balloon containing Ar is attached). Following the separation procedure described in the Supporting Information, the product was analyzed by means of the powder X-ray diffraction (XRD) pattern, which matched that of hexagonal Fe_2P (JCPDS card no. 85-1725; see Supporting Information, Figure S1). The absence of XRD peaks from metallic Fe indicated complete disappearance of the Fe phase. In addition, we could not observe the catalyst Pd phase by XRD.

The products were analyzed by transmission electron microscopy (TEM) and high-resolution TEM (HRTEM), as shown in Figure 1. Strikingly different Fe_2P nanorod products with different diameters and lengths could be obtained by varying only the diameter and the amount of employed Pd nanoparticles; other reaction parameters, namely, amount of Fe nanoparticle precursor and surfactants, reaction temperature, and solvent volume, were kept constant. Short nanorods (Figure 1a, c, and e) are obtained with a large Pd/Fe

[*] H. Kim, Y. Chae, M. Kim, J. Huh, Y. Kim, H. Kim, H. J. Kim, Prof. K. Choi, Prof. J. S. Kim, Prof. K. Lee
Department of Chemistry, Korea University
Seoul 136-701 (Korea)
E-mail: kylee1@korea.ac.kr
Homepage: http://nanolab.korea.ac.kr
D. H. Lee, Prof. S. O. Kim
Department of Material Science and Engineering,
Korea Advanced Institute of Science and Technology
Daejon, 305-701 (Korea)
E-mail: sangouk.kim@kaist.ac.kr
Dr. H. Baik
Korea Basic Science Institute (KBSI)
Seoul 136-713 (Korea)
Prof. G.-R. Yi
Department of Industrial Engineering Chemistry,
Chungbuk University
Cheongju, 361-763 (Korea)

[**] This work was supported by MEST (NRF 2009-0090897, KRF-2008-314-C00234, NRF 2010-0014807) and MIHWAF (the Korea Health 21 R&D Project: A085136) to K.L., by the NRL program (R0A-2008-000-20057-0) to S.O.K., and by NRF 2009-0082451 to G.R.Y. We thank KBSI for allowing the usage of their HRTEM, SQUID, GC-MS (operator: Yun Gyong Ahn) instruments and Prof. Sang-Won Lee at Korea Univ for MS measurements.

Supporting information for this article is available on the WWW under http://dx.doi.org/10.1002/anie.201001822.

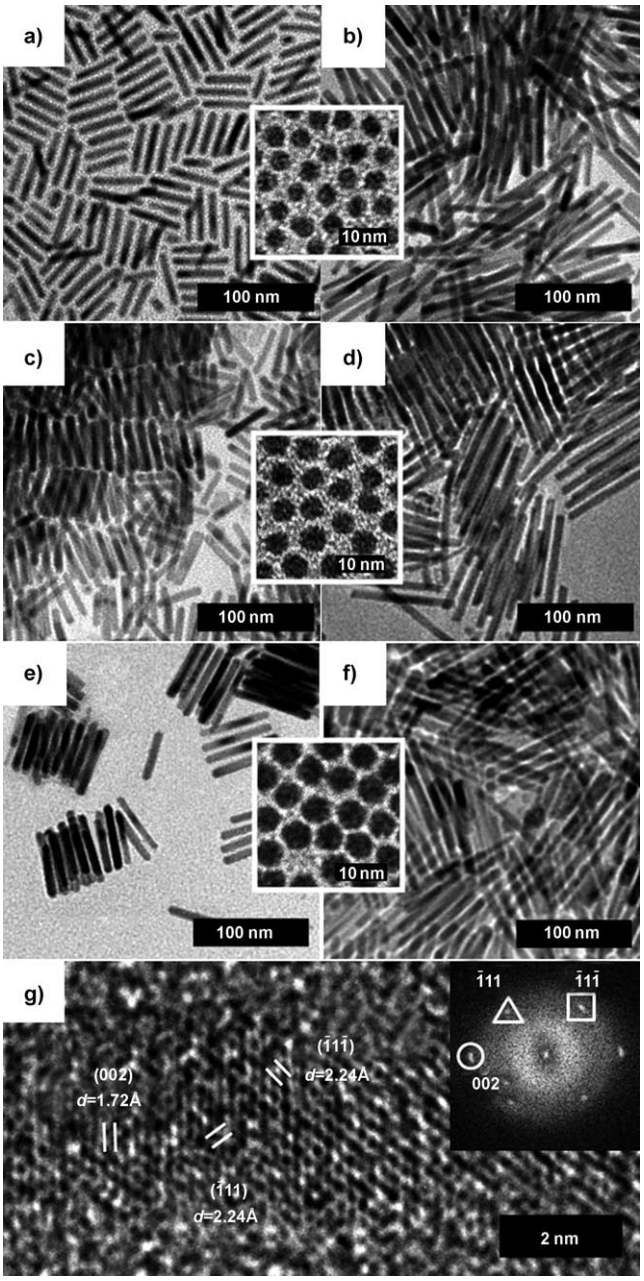

Figure 1. TEM images of a) $(5.7\times36.5)\pm(0.7\times3.5)$ nm, b) $(6.6\times66.2)\pm(1.0\times10.1)$ nm, c) $(6.2\times43.8)\pm(0.5\times4.2)$ nm, d) $(7.7\times90.2)\pm(1.0\times8.2)$ nm, e) $(7.4\times49.4)\pm(1.5\times5.6)$ nm, and f) $(9.6\times106.6)\pm(1.9\times12.2)$ nm Fe_2P nanorods. (Inset: TEM images of 3.5 ± 0.3, 4.2 ± 0.3, and 4.9 ± 0.3 nm Pd nanoparticles used as catalysts). g) High-resolution TEM image and accompanying fast Fourier transform image (inset) of a Fe_2P nanorod in (e) along $\langle110\rangle$.

ratio, and long nanorods (Figure 1 b,d, and f) with a small Pd/Fe ratio. This suggests that the number of formed nanorods is proportional to the number of employed Pd nanoparticles, not the number of Fe nanoparticles. Notably, the Fe_2P nanorod diameter is uniform within a batch and it is similar to the diameter of the employed Pd nanoparticles. The nanorods exhibit a core/shell-like structure in which a crystalline Fe_2P core with $\langle002\rangle$ growth direction (Figure 1 g) is covered by an amorphous shell with high phosphorus content (see Supporting Information, Figures S2 and S3 for TEM images showing the presence of a shell, as well as the shell composition). The diameters of the crystalline Fe_2P part in short nanorods (Figure 1 a, c, and e) are 3.7 ± 0.2, 4.4 ± 0.3, and 5.1 ± 0.3 nm, respectively, while the corresponding values for long nanorods (Figure 1 b, d, and f) are 4.2 ± 0.4, 4.7 ± 0.4, and 5.3 ± 0.3 nm, respectively (see Supporting Information, Table S1). The strong correlation between nanorod diameter and the Pd nanoparticle diameter is evident. This firmly supports that Pd nanoparticle acted as a catalytic center for Fe_2P nanorod growth. Such diameter control has been previously observed in vapor–liquid–solid (VLS)[13] and solution–liquid–solid (SLS)[14] methods, in which a catalytic nanoparticle is melted under the employed conditions and is found at the tip of the 1D nanostructure after the reaction. The Pd metal used in this study, however, has a high melting point of 1445 °C. Furthermore, a Pd nanoparticle was not observed on the tip of the formed Fe_2P nanorod despite the evident role of a Pd nanoparticle in determining the diameter of the nanorod.

Close examination of a fully grown 9.9×103.2 nm Fe_2P nanorod by an energy-dispersive X-ray spectroscopic (EDS) profile analysis revealed that Pd is found over the entire nanorod length, while the central part of the nanorod contains the most Pd (see Supporting Information, Figure S4). Localization of Pd content was not observed in this case, that is, the reaction mechanism is drastically different from those of typical VLS or SLS methods with an intact catalyst part. Thus, to fully understand the role of Pd nanoparticles in controlling Fe_2P nanorod dimensions, we obtained temporal TEM images of the reaction mixture and analyzed the elemental contents in various parts of growing nanorods (Supporting Information, Figure S5). Initially, core/shell nanoparticles with the Pd content confined to the core part are produced (Supporting Information, Figure S5a). Disappearence of all Fe nanoparticles even at this early stage indicates accelerated decomposition of the Fe phase by Pd nanoparticle based catalysis. The Pd-rich core now contains a significant amount of Fe and P, and the shell, richer in P than the core, is completely devoid of Pd. The diameter of the core is larger than that of the employed Pd nanoparticles diameter due to incorporation of Fe and P, which may also be responsible for the slightly larger diameter (core part) of Fe_2P nanorods compared to the used Pd nanoparticles.

The ability of Pd to dissolve Fe was previously demonstrated by formation of Fe–Pd alloy nanoparticle systems with various compositions, such as FePd, $FePd_2$, $FePd_3$, and $FePd_4$.[15] Thus, dissolution of Fe species in Pd nanoparticles to give an Fe–Pd alloy in our study can be understood. The Fe–Pd alloy with the highest Fe content appears to be FePd, because FePd coexists with Fe when the Fe content is in excess.[15b] When excess Fe precursors are dissolved into the alloy system, the Fe phase can precipitate from the supersaturated Fe–Pd alloy, reminiscent of a VLS mechanism. The precipitated Fe phase would rapidly react with P-donating species such as PH_3 formed in situ (vide infra) to form Fe_2P. Consistent with this mechanistic view, the core/shell nanoparticles, initially with an ellipsoidal shape, initiate preferential growth along the nanorod axis (see Supporting

Information, Figure S5b). Once nanorod growth starts, the diameter of the nanorod does not change significantly. The most striking feature of Fe_2P nanorod growth is that the Pd content is found throughout the nanorod structure, even when a nanorod grows longer (see Supporting Information, Figure S4). This clearly indicates that the core Fe–Pd system is slowly disintegrated, and the released Pd content is assimilated into the growing iron phosphide phase. Because Pd can also form various palladium phosphide phases, mixing of the Pd content, likely in the form of palladium phosphide, with the Fe_2P phase is not unexpected. The different reactivities of Pd and Fe toward P, as well as the relative abundance of Fe, seem to direct faster reaction between elemental Fe and P and thus fast outgrowth of Fe_2P nanorods. The slow disintegration of the Pd-rich alloy system in the middle of growing nanorods ensures the persistent presence of a catalytically active Pd-rich alloy in the middle of a growing nanorod throughout the reaction, continued intake of Fe content, precipitation of supersaturated Fe, and subsequent (or simultaneous) formation of the Fe_2P phase. It appears that the Pd-rich part in the middle of a growing nanorod could serve as a catalytically active growth center even with a much reduced Pd content until the later stage of reaction, because morphologies of nanorods obtained in our study are very homogeneous; if other competing pathways of nanorod formation are also operating in the later stage, irregularly shaped nanoparticles or nanorods would also appear, which is not the case in our study.

While all nanorod samples shown in Figure 1 exhibit XRD patterns typical of Fe_2P, short nanorods have a lower Fe/P ratio than long nanorods. For example, 6.2×43.8 nm nanorods with a core diameter of 4.4 nm (Figure 1c) and 7.7×90.2 nm nanorods with core diameter of 4.7 nm (Figure 1d), both formed in a reaction catalyzed by 4.2 nm Pd nanoparticles, exhibit Fe/P ratios of 1.6 and 2.4, respectively, as determined by electron-probe micro-analysis (see Supporting Information, Table S2, and also Figure S6 for EDS results). Short nanorods have a higher Pd content (2 vs. 0.25 atom % in long nanorods), and this results in significant differences in the final Fe and P contents in the nanorod structures. X-ray photoelectron spectroscopic analysis also suggests the presence of a P-rich phase such as FeP in the short nanorods with higher Pd content (see Supporting Information, Figure S7). Pd seems to take up more P than Fe, which prefers the formation of low-P phases like Fe_2P under the reaction conditions (note the initial ellipsoidal nanoparticle with a very high P content). In the early stage of nanorod formation from an Fe–Pd alloy with high Pd content, the Fe/P ratio is inevitably much lower than the expected value of 2. On the other hand, the composition of the core Fe_2P nanorods should exhibit a higher Fe/P ratio than the above measured values, because the formed nanorods are covered by an amorphous layer rich in P. Phases with a higher Fe content such as Fe or Fe_3P, even if unidentifiable through TEM or XRD analysis, might result in higher blocking temperatures of Fe_2P nanorods than expected for a pure Fe_2P phase (see Supporting Information, Figure S8 for magnetism measurements). Usage of Pd nanoparticles with diameters over 5.5 nm led to the competitive formation of platelike Fe_2P nanostructures besides nanorods (Supporting Information, Figure S9). The preferential growth of Fe_2P nanorods along $\langle 002 \rangle$ obviously is not entirely viable with larger Pd nanoparticles.

Under the same reaction conditions but without Pd nanoparticles, Fe nanoparticles reacted with TOP to form an uncontrolled mixture of nanoparticles and nanorods with Fe, FeP, and Fe_2P phases (Supporting Information, Figure S10). Obviously, Pd nanoparticles are essential for fast consumption of Fe nanoparticles in an early stage and ensuing formation of size- and composition-controlled Fe_2P nanorods. In our previous study, we suggested that soluble Pd^0 species can catalyze the reduction of Fe cations to form soluble iron species.[9] Thus we attempted the formation of Fe_2P nanorods with Fe_3O_4 nanoparticles as starting material. As expected, Pd nanoparticles could convert Fe_3O_4 nanoparticles to size-controlled Fe_2P nanorods. In this case, however, hollow spheres were also observed as side products (Supporting Information, Figure S11). Once an insoluble amorphous {Fe, P} layer is formed on a crystalline Fe_3O_4 nanoparticle, it cannot be assimilated into a Pd nanoparticle. This precludes its conversion to Fe_2P, and thus the amorphous shell remains stable under the reaction conditions. In the case of Fe nanoparticle as a precursor, the surface Fe atoms can also be easily oxidized (see Supporting Information, Figure S12). The oxide phase on a Fe nanoparticle, however, is not crystalline, and thus dissolution of this amorphous oxide phase is too fast to support the formation of an amorphous {Fe, P} layer. Due to this stability difference between crystalline and amorphous iron oxide phases, we observe no hollow spheres as side products with Fe nanoparticle precursors.

We noticed that the amount of OA in the reaction mixture decreases (GC-MS analysis; Supporting Information, Figure S10) with formation of $C_{54}H_{97}N$ (Supporting Information, Figures S13 and S14) during Fe_2P nanorod formation; a drastic decrease of OA was observed only under conditions in which Fe_2P nanorods are successfully prepared. We could not detect the presence of non-amine functional groups such as CN in NMR and IR spectroscopic data for $C_{54}H_{97}N$. Thus, we carried out a series of amine tests[16] and ruled out the possibility of this $C_{54}H_{97}N$ species being a primary or secondary amine, leaving a tertiary amine with unsaturated hydrocarbon chains as the most likely candidate structure for $C_{54}H_{97}N$ (see Supporting Information, Figure 15). Without Fe nanoparticles, a Pd nanoparticle alone could not form this $C_{54}H_{97}N$ compound. In addition, Fe_2P nanorods obtained from our study could not catalyze the formation of tertiary amine species under the reaction conditions. Interestingly, formation of $C_{54}H_{97}N$ is also accompanied by formation of NH_3. It has been shown that OA can be decomposed to form NH_3 in the presence of cobalt species.[17] Thus, iron species generated in situ may have catalyzed the formation of $C_{54}H_{97}N$ by decomposition of OA with concomitant formation of NH_3.

The complete absence of Ar flow was crucial for the formation of Fe_2P nanorods from Fe or Fe_3O_4 nanoparticles. Even with an Ar flow rate of 10 $cm^3 min^{-1}$, no Fe_2P nanorods could be synthesized (see Supporting Information, Figure S10). Because an Ar stream can easily deplete in situ generated volatile species such as NH_3 and PH_3, which were

detected by a gas sensor, from the reaction mixture, the role of volatile species was probed by a series of reactions (see Supporting Information, Figure S16). With an NH_3 stream of 10 $cm^3 min^{-1}$, volatile components other than NH_3 would be removed from the reaction mixture. No Fe_2P nanorod could be obtained under these conditions. We then investigated the role of PH_3, formed by decomposition of TOP (likely following elimination of octene), in the formation of Fe_2P nanorods. Again, no Fe_2P nanorod was obtained with a PH_3 flow (10 $cm^3 min^{-1}$, 5 vol% in Ar), in which NH_3 in situ generated would be removed from the reaction mixture. Under these conditions, large iron nanoparticles disappeared following Fe nanoparticle dissolution, and small wormlike nanoparticles of FeP formed by attachment of small FeP nanoparticles were observed; clearly, Pd nanoparticles did not serve as catalytic centers for fast growth of Fe_2P nanorods in this case. Only when both NH_3 and PH_3 (5% v/v in Ar) gases were introduced simultaneously at respective flow rates of 7 and 15 $cm^3 min^{-1}$ could nanorods of Fe_2P be obtained. Thus, it seems that PH_3 formed in situ is necessary for conversion of Fe to Fe_2P, and NH_3 for activation of the Pd nanoparticle catalyst. Since excess PH_3 can deactivate the Pd nanoparticle by binding strongly to its surface, a large amount of weakly binding NH_3 may, by competing with the PH_3 ligands, allow influx of soluble Fe species into the Pd matrix. The presence of a large amount of O_2 was detrimental to the formation of Fe_2P nanorods; no Fe_2P nanorod formation was observed when the reaction mixture was blanketed by 10 vol% O_2 in Ar (1 atm, balloon; see Supporting Information, Figure S16). Oxygen may interfere with Fe_2P formation by effectively removing pyrophoric PH_3 from the reaction mixture. Thus, the additional role of PH_3 in the Fe_2P nanorod synthesis may lie in maintaining the reducing environment by effectively removing traces of oxygen, which could be introduced by diffusion, from the reaction mixture. The total absence of Ar flow and presence of pyrophoric PH_3 provide a completely oxygen-free environment, which might be essential for Fe_2P nanorod growth.

To further substantiate the catalytic role of a Pd nanoparticle in the growth of a Fe_2P nanorod, we prepared an ordered 2D array of approximately 7 nm Pd nanoparticles on an Si substrate,[18] and attempted the growth of Fe_2P nanorods thereon (see Supporting Information for experimental details, and Figures S17 and S18). Consistent with our prediction, we could grow Fe_2P nanorods from Pd nanoparticles supported on an Si substrate (Figure 2). The diameter of the Fe_2P nanorods is slightly larger than that of the Pd nanoparticles (10–15 nm, see Figure 2d; note that the top view Figure 2b selectively shows only thicker nanorods), consistent with solution-based results. On the other hand, Fe_2P nanorods could not grow on a clean Si substrate without Pd, in further corroboration of the crucial role of Pd as catalytic center for Fe_2P nanorod growth. The overall Fe_2P nanorod growth process is depicted in Figure 3.

In summary, we have reported a novel Pd nanoparticle catalyzed synthesis of diameter-specific and length-controlled Fe_2P nanorods from Fe nanoparticles. The diameter and length of Fe_2P nanorods could be finely controlled by adjusting the size of the catalytic Pd nanoparticles and the Fe/Pd ratio, respectively, and this in turn allows magnetic properties to be fine-tuned. Such controllable magnetic properties could be useful in future magnetic-device applications. The Pd nanoparticles perform a dual role as catalyst destabilizing the Fe phase and catalytic center for Fe_2P nanorod growth. The Fe nanoparticles are completely disintegrated under the employed reaction conditions to form a new Fe precursor, unavailable via other routes, which is ultimately converted to Fe_2P nanorods. The excess Fe content, likely to have precipitated from a supersaturated Fe–Pd alloy system, combines with P from active P sources such as PH_3, formed in situ, to form Fe_2P. We are currently investigating the possible transformation of existing nanomaterials into hitherto-unknown precursors catalyzed by Pd or other noble metals. Our approach would eventually provide a number of novel nanomaterials with better dimensional control and reproducible material properties.

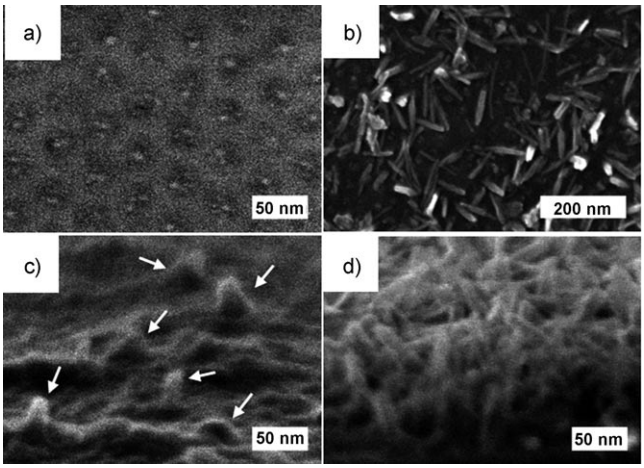

Figure 2. Fe_2P nanorod growth on an Si-supported Pd substrate. SEM images of a) an array of approximately 7 nm Pd nanoparticles on Si. b) Fe_2P nanorods grown on an Si substrate at a reaction time of 5 h (top view). c) Side view of swollen Pd nanoparticles due to solid-solution formation and short nanorods (indicated with arrows) at a reaction time of 3 h. d) Side view of Fe_2P nanorods grown vertically on an Si substrate.

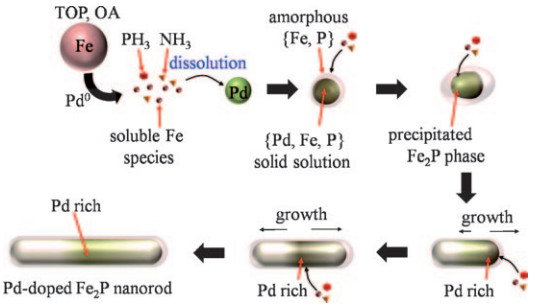

Figure 3. Fe_2P nanorod growth process.

Received: March 27, 2010
Revised: May 20, 2010
Published online: July 2, 2010

Keywords: crystal growth · iron · nanoparticles · nanostructures · palladium

[1] a) A. R. Tao, S. Habas, P. Yang, *Small* **2008**, *4*, 310 – 325; b) Y. Yin, A. P. Alivisatos, *Nature* **2005**, *437*, 664 – 670.

[2] a) J. Maynadié, A. Salant, A. Falqui, M. Respaud, E. Shaviv, U. Banin, K. Soulantica, B. Chaudret, *Angew. Chem.* **2009**, *121*, 1846 – 1849; *Angew. Chem. Int. Ed.* **2009**, *48*, 1814 – 1817; b) K. H. Park, K. Jang, H. J. Kim, S. U. Son, *Angew. Chem.* **2007**, *119*, 1170 – 1173; *Angew. Chem. Int. Ed.* **2007**, *46*, 1152 – 1155; c) J. Park, K. An, Y. Hwang, J.-G. Park, H.-J. Noh, J.-Y. Kim, J.-H. Park, N.-M. Hwang, T. Hyeon, *Nat. Mater.* **2004**, *3*, 891 – 895.

[3] a) S. Sapra, J. Poppe, A. Eychmüller, *Small* **2007**, *3*, 1886 – 1888; b) G. Wang, W. Lu, J. Li, J. Choi, Y. Jeong, S.-Y. Choi, J.-B. Park, M. K. Ryu, K. Lee, *Small* **2006**, *2*, 1436 – 1439; c) C. H. Lee, M. Kim, T. Kim, A. Kim, J. Paek, J. W. Lee, S.-Y. Choi, K. Kim, J.-B. Park, K. Lee, *J. Am. Chem. Soc.* **2006**, *128*, 9326 – 9327; d) K. Lee, W. S. Seo, J. T. Park, *J. Am. Chem. Soc.* **2003**, *125*, 3408 – 3409; e) Y.-W. Jun, S.-M. Lee, N.-J. Kang, J. Cheon, *J. Am. Chem. Soc.* **2001**, *123*, 5150 – 5151.

[4] a) B. Sadtler, D. O. Demchenko, H. Zheng, S. M. Hughes, M. G. Merkle, U. Dahmen, L.-W. Wang, A. P. Alivisatos, *J. Am. Chem. Soc.* **2009**, *131*, 5285 – 5293; b) R. D. Robinson, B. Sadtler, D. O. Demchenko, C. K. Erdonmez, L.-W. Wang, A. P. Alivisatos, *Science* **2007**, *317*, 355 – 358; c) P. H. C. Camargo, Y. H. Lee, U. Jeong, Z. Zou, Y. Xia, *Langmuir* **2007**, *23*, 2985 – 2992; d) D. H. Son, S. M. Hughes, Y. Yin, A. P. Alivisatos, *Science* **2004**, *306*, 1009 – 1012.

[5] a) C. Wang, H. Daimon, T. Onodera, T. Koda, S. Sun, *Angew. Chem.* **2008**, *120*, 3644 – 3647; *Angew. Chem. Int. Ed.* **2008**, *47*, 3588 – 3591; b) D. Seo, J. C. Park, H. Song, *J. Am. Chem. Soc.* **2006**, *128*, 14863 – 14870.

[6] a) H. G. Yang, C. H. Sun, S. Z. Qiao, J. Zou, G. Liu, S. C. Smith, H. M. Cheng, G. Q. Lu, *Nature* **2008**, *453*, 638 – 641; b) F. Tao, M. E. Grass, Y. Zhang, D. R. Butcher, J. R. Renzas, Z. Liu, J. Y. Chung, B. S. Mun, M. Salmeron, G. A. Somorjai, *Science* **2008**, *322*, 932 – 934; c) P. Nolte, A. Stierle, N. Y. Jin-Phillipp, N. Kasper, T. U. Schulli, H. Dosch, *Science* **2008**, *321*, 1654 – 1658.

[7] a) B. Lim, M. Jiang, P. H. C. Camargo, E. C. Cho, J. Tao, X. Lu, Y. Zhu, Y. Xia, *Science* **2009**, *324*, 1302 – 1305; b) B. Lim, J. Wang, P. H. C. Camargo, M. Jiang, M. J. Kim, Y. Xia, *Nano Lett.* **2008**, *8*, 2535 – 2540; c) D. Seo, C. I. Yoo, J. Jung, H. Song, *J. Am. Chem. Soc.* **2008**, *130*, 2940 – 2941; d) S. E. Habas, H. Lee, V. Radmilovic, G. A. Somorjai, P. Yang, *Nat. Mater.* **2007**, *6*, 692 – 697.

[8] a) M. Schrinner, M. Ballauff, Y. Talmon, Y. Kauffmann, J. Thun, M. Möller, J. Breu, *Science* **2009**, *323*, 617 – 620; b) B. Lim, X. Lu, M. Jiang, P. H. C. Camargo, E. C. Cho, E. P. Lee, Y. Xia, *Nano Lett.* **2008**, *8*, 4043 – 4047; c) N. Tian, Z.-Y. Zhou, S.-G. Sun, Y. Ding, Z. L. Wang, *Science* **2007**, *316*, 732 – 735; d) X. Lu, L. Au, J. McLellan, Z.-Y. Li, M. Marquez, Y. Xia, *Nano Lett.* **2007**, *7*, 1764 – 1769; e) D. Kim, J. Park, K. An, N.-K. Yang, J.-G. Park, T. Hyeon, *J. Am. Chem. Soc.* **2007**, *129*, 5812 – 5813.

[9] H. Kim, M. Lee, Y. Kim, J. Huh, H. Kim, M. Kim, T. Kim, V. N. Phan, Y.-B. Lee, G.-R. Yi, S. Haam, K. Lee, *Angew. Chem.* **2009**, *121*, 5231 – 5235; *Angew. Chem. Int. Ed.* **2009**, *48*, 5129 – 5133.

[10] a) E. Muthuswamy, P. R. Kharel, G. Lawes, S. L. Brock, *ACS Nano* **2009**, *3*, 2383 – 2393; b) A. T. Kelly, I. Rusakova, T. Ould-Ely, C. Hofmann, A. Lüttge, K. H. Whitmire, *Nano Lett.* **2007**, *7*, 2920 – 2925; c) J. Park, B. Koo, K. Y. Yoon, Y. Hwang, M. Kang, J.-G. Park, T. Hyeon, *J. Am. Chem. Soc.* **2005**, *127*, 8433 – 8440; d) C. Qian, F. Kim, L. Ma, F. Tsui, P. Yang, J. Liu, *J. Am. Chem. Soc.* **2004**, *126*, 1195 – 1198; e) J. Park, B. Koo, Y. Hwang, C. Bae, K. An, J.-G. Park, H. M. Park, T. Hyeon, *Angew. Chem.* **2004**, *116*, 2332 – 2335; *Angew. Chem. Int. Ed.* **2004**, *43*, 2282 – 2285.

[11] a) S. Peng, S. Sun, *Angew. Chem.* **2007**, *119*, 4233 – 4236; *Angew. Chem. Int. Ed.* **2007**, *46*, 4155 – 4158; b) S. Peng, C. Wang, J. Xie, S. Sun, *J. Am. Chem. Soc.* **2006**, *128*, 10676 – 10677.

[12] S.-W. Kim, J. Park, Y. Jang, Y. Chung, S. Hwang, T. Hyeon, *Nano Lett.* **2003**, *3*, 1289 – 1291.

[13] J. Hu, T. W. Odom, C. M. Lieber, *Acc. Chem. Res.* **1999**, *32*, 435 – 445.

[14] a) S. P. Ahrenkiel, O. I. Mićić, A. Miedaner, C. J. Curtis, J. M. Nedeljković, A. J. Nozik, *Nano Lett.* **2003**, *3*, 833 – 837; b) S. Kan, T. Mokari, E. Rothenberg, U. Banin, *Nat. Mater.* **2003**, *2*, 155 – 158; c) T. J. Trentler, S. C. Goel, K. M. Hickman, A. M. Viano, M. Y. Chiang, A. M. Beatty, P. C. Gibbons, W. E. Buhro, *J. Am. Chem. Soc.* **1997**, *119*, 2172 – 2181.

[15] a) M.-H. Shao, K. Sasaki, R. R. Adzic, *J. Am. Chem. Soc.* **2006**, *128*, 3526 – 3527; b) T. Teranishi, A. Wachi, M. Kanehara, T. Shoji, N. Sakuma, M. Nakaya, *J. Am. Chem. Soc.* **2008**, *130*, 4210 – 4211.

[16] J. S. Kim, S. J. Lee, J. H. Jung, I.-C. Hwang, N. J. Singh, S. K. Kim, S. H. Lee, H. J. Kim, C. S. Keum, J. W. Lee, K. S. Kim, *Chem. Eur. J.* **2007**, *13*, 3082 – 3088.

[17] K. M. Nam, J. H. Shim, H. Ki, S.-I. Choi, G. Lee, J. K. Jang, Y. Jo, M.-H. Jung, H. Song, J. T. Park, *Angew. Chem.* **2008**, *120*, 9646 – 9650; *Angew. Chem. Int. Ed.* **2008**, *47*, 9504 – 9508.

[18] a) D. H. Lee, W. J. Lee, S. O. Kim, *Nano Lett.* **2009**, *9*, 1427 – 1432; b) D. H. Lee, D. O. Shin, W. J. Lee, S. O. Kim, *Adv. Mater.* **2008**, *20*, 2480 – 2485.

